Pseudostate calculations in n+t and p+^{3}He systems

P. N. Shen and Y. C. Tang
School of Physics, University of Minnesota, Minneapolis, Minnesota 55455

H. Kanada and T. Kaneko
Department of Physics, Niigata University, Niigata 950-21, Japan

(Received 25 November 1985)

The specific distortion effect of the three-nucleon cluster in the n+t or p+^{3}He system is studied by using the pseudostate method in the resonating-group formulation. The result indicates that such an effect is significant mainly at low energies around the broad resonance in the Pauli-favored $l=1$ state. In the higher-energy region, a comparison between differential cross sections calculated with and without distortion shows that this effect has only a minor influence.

I. INTRODUCTION

The pseudostate method[1] has been used to study specific distortion effects in resonating-group calculations of light $A+B$ systems. As was summarized in Ref. 2, the results from p+α (Ref. 3), d+α (Ref. 4), t+α (Ref. 5), and $\alpha+\alpha$ (Ref. 6) studies showed that such effect is strong in the d+α case, moderate in the t+α case, but comparatively less important in the p+α and $\alpha+\alpha$ cases. This indicates that the importance of specific distortion is closely related to the degree of compressibility of the clusters involved in the system.

The purpose of this investigation is to examine the manner in which the nature of the companion cluster B influences the effect caused by the specific distortion of the cluster A. To achieve this purpose, we shall consider the light system n + t or p+^{3}He. By comparing the obtained results with those reported previously in the t+α case, one can then gain information concerning the degree in which the specific distortion of the t cluster depends on the nucleon number of the companion cluster which is a single nucleon in the n + t case, but a heavier α cluster in the t+α case.

In the next section, a brief description of the formulation is given. Convergence properties with respect to the required number of pseudostate configurations is discussed in Sec. III. Phase-shift results in the n + t case and differential cross-section results in the p+^{3}He case are presented in Sec. IV. Finally, in Sec. V, concluding remarks are made.

II. BRIEF DISCUSSION OF THE FORMULATION

The trial wave function for the system is taken to have the form

$$\Psi_s=\sum_{i=1}^{N}\mathcal{A}[\phi_i\xi_s F_{is}(\mathbf{R})Z(\mathbf{R}_{\text{c.m.}})]\ , \tag{1}$$

where $\mathcal{A}$ is the antisymmetrization operator, ξ_s is an appropriate spin-isospin function with the subscript s denoting the total spin angular momentum ($s=0,1$), $Z(\mathbf{R}_{\text{c.m.}})$ is any normalizable function describing the center-of-mass motion, and N is the number of configurations adopted in the calculation. The functions ϕ_1 and ϕ_i ($i=2$ to N) describe the internal spatial behavior of the three-nucleon cluster in its ground and pseudoexcited states, respectively. They are chosen to be

$$\phi_i=\sum_{j=1}^{n}A_{ij}\chi_j,\ \ i=1 \text{ to } N\ (N\le n)\ , \tag{2}$$

where n denotes the number of basis functions χ_j. These latter functions are assumed as

$$\chi_j=\exp\left[-\tfrac{1}{2}\alpha_j\sum_{k=1}^{3}(\mathbf{r}_k-\mathbf{R}_3)^2\right]\ , \tag{3}$$

with $\mathbf{R}_3$ representing the c.m. coordinate of the three-nucleon cluster. It should be mentioned that the pseudoexcited states are constructed to yield pseudoinelastic configurations which are used to describe the specific distortion effect in the n + t or p+^{3}He system.

For a given value of n, the nonlinear parameters α_j ($j=1$ to n) are chosen by minimizing the ground-state expectation value $\tilde{E}_1$ of the three-nucleon Hamiltonian. With the resultant values of α_j, the coefficients A_{ij} are then determined by diagonalizing the Hamiltonian matrix in the restricted space spanned by the nonorthonormal Gaussian basis functions χ_j. The results for α_j and A_{ij} in the triton case are tabulated in Tables I and II, respectively. In Table II, we have additionally listed also the values of the corresponding energies $\tilde{E}_i$ and rms matter radii $\tilde{R}_i$.

As a comparison, we have also computed $\tilde{E}_1$ and $\tilde{R}_1$ in a model space spanned by a large number of Gaussian basis functions ($n=15$). Results obtained with several appropriately chosen sets of α_j values, ranging from 0.05 to 7.5 fm^{-2}, turn out to be nearly identical. These results are

$$\tilde{E}_1=-6.031 \text{ MeV},\ \ \tilde{R}_1=1.697 \text{ fm}\ . \tag{4}$$

By comparing with the corresponding values in Table II, we note that the spatial structure of the triton cluster is well described when n is chosen to be larger than or equal to 4.

TABLE I. Nonlinear variational parameters α_j of the triton.

n	α_1 (fm^{-2})	α_2 (fm^{-2})	α_3 (fm^{-2})	α_4 (fm^{-2})	α_5 (fm^{-2})	α_6 (fm^{-2})
1	0.454					
2	0.191	0.641				
3	0.205	0.691	4.264			
4	0.131	0.370	0.903	3.279		
5	0.105	0.285	0.675	1.407	2.932	
6	0.0815	0.208	0.500	1.181	1.991	3.646

The relative-motion functions or variational amplitudes $F_{is}(\mathbf{R})$ are determined by solving the projection equation

$$\langle \delta\Psi_s \mid H - E_T \mid \Psi_s \rangle = 0 , \tag{5}$$

where

$$E_T = \tilde{E}_i + E_i, \quad (i = 1 \text{ to } N) \tag{6}$$

with E_T being the total energy of the system and E_i being the relative energy of the neutron and the triton cluster in the ith configuration (E_1 in the elastic channel will be simply written as E in the following discussion). The Hamiltonian operator H is given by

$$H = -\frac{\hbar^2}{2M}\sum_{i=1}^{4}\nabla_i^2 + \sum_{i>j=1}^{4} V_{ij} - T_{\text{c.m.}} , \tag{7}$$

where $T_{\text{c.m.}}$ is the kinetic-energy operator of the total c.m. motion and $\hbar^2/2M$ is equal to 20.735 MeV fm^2. The nucleon-nucleon potential V_{ij} (hereafter referred to as the MN potential) is assumed to be purely central and has the form given by Eqs. (9)–(11) in Ref. 6. The exchange-mixture parameter u is taken to be 1. This particular value is chosen, because it has been found recently[7] that, with specific distortion properly taken into account, the MN potential with this u value can be used to achieve a satisfactory description of the main features of many light nuclear systems.

By following the standard resonating-group procedure,[8] coupled integrodifferential equations for F_{is} are derived. These equations are solved by using a variational technique discussed by Kamimura.[9] From the solutions, one obtains the S-matrix elements and, subsequently, the elastic-scattering phase shifts δ_l and the differential scattering cross sections $\sigma(\theta)$.

III. DETERMINATION OF REQUIRED NUMBERS OF BASIS FUNCTIONS AND PSEUDOINELASTIC CONFIGURATIONS

Our initial task is to determine the number $(N-1)$ of pseudoinelastic configurations required for convergence

TABLE II. Variational results for triton configurations.

n	i	A_{i1}	A_{i2}	A_{i3}	A_{i4}	A_{i5}	A_{i6}	$\tilde{E}_i$ (MeV)	$\tilde{R}_i$ (fm)
1	1	0.1252						−4.558	1.484
2	1	0.017 38	0.1281					−5.859	1.680
	2	−0.038 80	0.2278					12.568	2.250
3	1	0.020 65	0.1370	−0.084 77				−5.975	1.663
	2	−0.042 60	0.2628	−0.1328				13.999	2.148
	3	0.006 804	−0.1008	3.8708				283.893	0.615
4	1	0.005 479	0.048 90	0.1231	−0.096 68			−6.028	1.690
	2	−0.024 97	0.077 98	0.058 65	−0.038 51			6.538	2.964
	3	0.015 07	−0.1860	0.6224	−0.3329			37.561	1.919
	4	−0.004 386	0.066 60	−0.3971	3.1772			246.010	0.801
5	1	0.002 659	0.028 89	0.096 21	0.074 28	−0.1199		−6.030	1.695
	2	−0.018 40	0.048 67	0.010 33	0.1133	−0.1162		4.702	3.385
	3	0.012 89	−0.1458	0.4521	−0.1887	0.043 59		25.116	2.384
	4	−0.006 422	0.1046	−0.7768	2.1701	−1.3585		88.070	1.537
	5	0.002 925	−0.049 46	0.4590	−2.1398	4.8319		302.461	0.856
6	1	0.001 025	0.014 21	0.071 22	0.1334	−0.073 77	−0.065 44	−6.031	1.697
	2	0.012 68	−0.025 83	−0.003 882	−0.1353	0.1220	−0.017 15	3.339	3.882
	3	0.010 07	−0.093 47	0.2485	−0.1552	0.3232	−0.2870	16.832	2.872
	4	−0.005 172	0.070 66	−0.4823	1.9165	−1.7765	0.6380	59.186	1.894
	5	0.002 691	−0.039 33	0.3605	−3.0460	6.6496	−3.7723	168.652	1.246
	6	−0.001 445	0.020 99	−0.2026	2.2013	−6.9210	9.8446	455.657	0.759

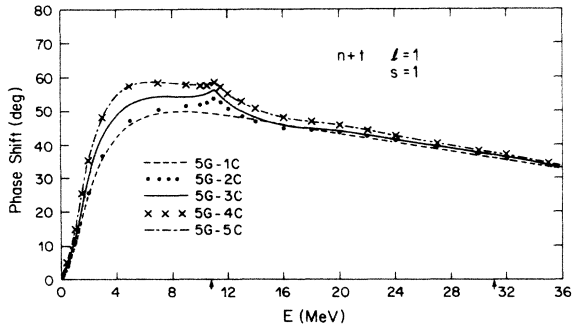

FIG. 1. Phase shifts in the $(l,s)=(1,1)$ state of n + t scattering calculated in the five-Gaussian case with 1, 2, 3, 4, and 5 cluster configurations. Arrows on the abscissa mark the energy thresholds of pseudoinelastic configurations.

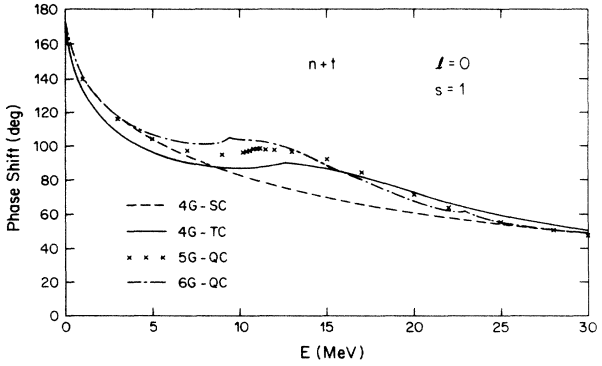

FIG. 3. Phase shifts in the $(l,s)=(0,1)$ state of n + t scattering calculated with different numbers of Gaussian basis functions.

and the number n of Gaussian basis functions necessary for accuracy. Smallest possible values of n and N will be adopted in the final calculation, because lengthy computational periods are needed in this investigation.

First, we consider the question concerning the required number N of cluster configurations. For this purpose, we compute, for a given choice of n and in the Pauli-favored state with $(l,s)=(1,1)$, the phase shifts in a number of calculations adopting progressively larger numbers of pseudoinelastic configurations. The results for n + t scattering are illustrated in Fig. 1 in the case with five Gaussian basis functions (i.e., $n=5$ or $5G$ case). In this figure, the dashed curve, solid dots, solid curve, crosses, and dot-dashed curve represent the results obtained with 1, 2, 3, 4, and 5 cluster configurations, respectively (denoted in the figure as $1C$, $2C$, $3C$, $4C$, and $5C$ calculations). From this figure, one learns the effect of successively adding pseudoinelastic configurations with higher energy thresholds and finds that convergence is achieved with $N=4$ in this particular case. The phase-shift values obtained in the $4C$ and $5C$ calculations are seen to be almost identical. This is, in fact, to be expected, since the threshold energy of the pseudoinelastic configuration with ϕ_5 has a large value equal to 308.49 MeV and, hence, its influence on the n + t scattering phase shifts in the energy region of 0—36 MeV should be quite negligible.

Similar investigations have also been conducted in cases with $n=2$, 3, 4, and 6. Here we find that convergences are achieved at $N=2$, 2, 3, and 4, respectively. This indicates that, in the energy region studied here, pseudoinelastic configurations with energy thresholds higher than about 100 MeV make very little contribution, which is of course a rather reasonable finding.

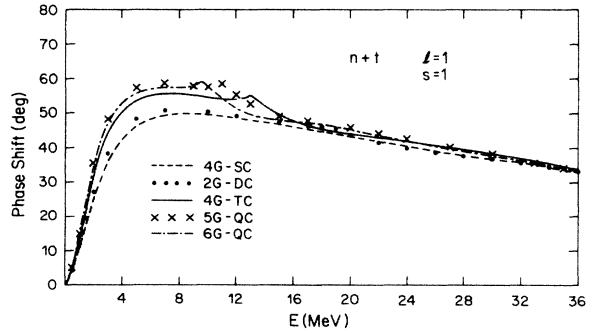

FIG. 2. Phase shifts in the $(l,s)=(1,1)$ state of n + t scattering calculated with different numbers of Gaussian basis functions.

Phase-shift results for n + t scattering in the $(l,s)=(1,1)$ state, obtained with $n=2$, 4, 5, and 6, are summarized in Fig. 2. In this figure, the dots, solid curve, crosses, and dot-dashed curve represent results obtained with double configurations (DC or $N=2$) in the $n=2$ case, triple configurations (TC or $N=3$) in the $n=4$ case, and quadruple configurations (QC or $N=4$) in the $n=5$ and 6 cases, respectively. In addition, we have also shown, as a comparison, the result from a single-configuration (SC) calculation[10] with $n=4$. From this figure, one notes that, except in the region where energy thresholds occur, the $4G$-TC, $5G$-QC, and $6G$-QC phase-shift results are rather similar to one another. This suggests that, for a general understanding of the effects of specific distortion in the n + t system, the adoption of a $4G$-TC calculation seems to be sufficient.

The above conclusion concerning the use of a $4G$-TC calculation has also been examined in the Pauli-unfavored $(l,s)=(0,1)$ state. In Fig. 3, we show the phase-shift results, obtained in the same cases as those in the $(l,s)=(1,1)$ state. Here one finds again that, at energies beyond the region containing the energy thresholds, the $5G$-QC result is rather similar to the $6G$-QC result. The $4G$-TC result is somewhat different; however, especially for energies higher than about 20 MeV, the difference is not too large. Therefore, for the sake of saving computational time, we have decided to use mainly the $4G$-TC model space in the remainder of the calculation.

IV. RESULTS

A. Phase shifts in the n + t system

Phase shifts for n + t scattering, calculated with $4G$-TC (solid curves) and $4G$-SC (dashed curves), are shown in Fig. 4 for $l=0-3$ in $s=0$ and 1 states. In this figure, the arrows on the abscissa mark the energy threshold of

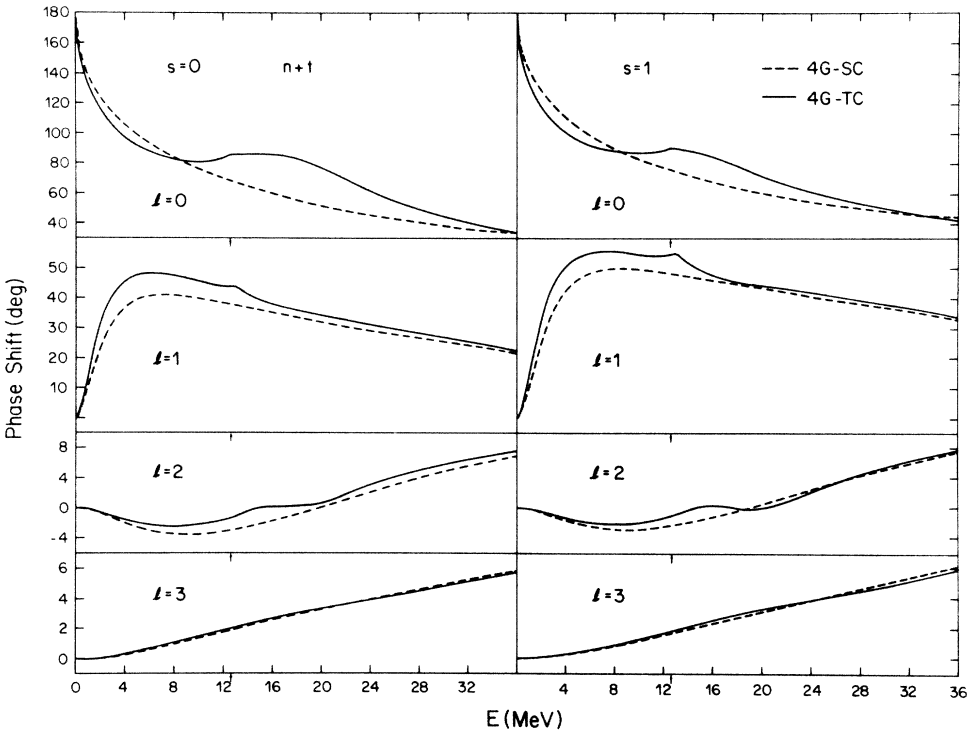

FIG. 4. Calculated phase shifts in various (l,s) states of the n + t system.

the lowest pseudoinelastic channel in the 4G-TC case. As is noted, the features in the $s=0$ and $s=1$ states are entirely similar. Hence, in the following discussion, we shall focus our attention only on the $s=1$ states.

The most notable features in Fig. 4 are that there occur cusps and dispersionlike resonances near the energy threshold. These are unphysical features which arise as a consequence of the introduction of pseudoinelastic channels into the calculation. Quite clearly, this represents a defect of the pseudostate method and has the consequence that, in this system, one can make a detailed comparison between calculated and experimental differential cross-section results only in the relatively high-energy region beyond about 20 MeV. To alleviate this defect, one could perform a more extensive calculation[4] by enlarging the model space through the use of larger values of n and N. This would, however, result in a considerable increase in computational periods. A better way is to carry out a more difficult calculation by introducing realistic reaction channels, such as the three-body n + n + d channel.

From previous investigations,[5,11] we have learned that specific distortion effects show up most distinctly in Pauli-favored orbital angular-momentum states. For the n + t system, the only such state is the $l=1$ state. Here one finds from Figs. 2 and 4 that the specific distortion has indeed a considerable influence on the energy position of the broad resonance level at around 4 MeV. With the 6G-QC calculation, the resonance energy is lowered by almost 0.9 MeV. In all other l states, however, one notes from Figs. 3 and 4 that, with the exclusion of the energy region in which nonphysical cusps and dispersionlike resonances occur, the effect of specific distortion of the triton cluster is quite minor.

Next, we compare the importance of triton distortion effects in the n + t and t+α systems. For this purpose, we study the phase-shift differences between with- and without-distortion results obtained at energies away from physical or nonphysical resonances in the Pauli-favored $l=1$ state. From Fig. 2, one finds that this difference in the n + t, 6G case at 20 MeV is about 2° which is considerably smaller than the difference of about 13° in the t+α case[5] at the same energy. To express this difference in another way, we have also computed the value of Δu, defined as

$$\Delta u = u_{\text{eff}} - u_0 \ , \tag{8}$$

where u_0 denotes the u value used in the with-distortion calculation and u_{eff} is the u value necessary to achieve, in a SC or no-distortion calculation, the same phase-shift value as that obtained in the with-distortion case. For the n + t system at 20 MeV, Δu is equal to about 0.04 which should be compared with the value of nearly 0.07 in the t+α case at this energy. From these comparisons, one can conclude that the nature of the companion cluster does have a considerable overall influence. The specific distortion effect in the t+α system is appreciably larger, simply because the companion α cluster contains a larger number of nucleons.

B. Differential scattering cross sections in the p+^{3}He system

Because of the presence of unphysical dispersionlike resonances, a comparison between calculation and experiment cannot be made at low energies. Therefore, in this subsection, we shall discuss the differential cross-section

results only in the higher-energy region from 22.5 to 35.625 MeV.

Differential cross-section values for the $p+^3He$ system are depicted in Figs. 5–7. In these figures, the solid and dashed curves represent results obtained from the $4G$-TC and $4G$-SC calculations, respectively, while the solid circles represent the experimental results.[12] From these figures, one notes the following features:

(i) The calculation explains all the essential features of the experimental data. In particular, the measured cross-section results in the backward angular region are well reproduced.

(ii) In the higher-energy region considered here, the specific distortion of the triton cluster seems to have only a minor effect. For example, differential cross sections at 22.5 MeV, calculated with and without specific distortion, differ by only 6.9% at 25° and 15.5% at 180°.

(iii) By comparing cross-section results obtained with and without distortion at various energies, one finds that the effect of specific distortion seems to decrease rather rapidly with increasing energy.

(iv) The calculated value of the differential cross section at the interference minimum near 120° is too small. This is quite clearly a consequence of the fact that noncentral forces are not included in the calculation.

The calculated angular position θ_{min} of the interference minimum in the cross-section curve agrees well with experimental finding. This is shown in Fig. 8. In this figure, one notes the interesting feature that θ_{min} becomes larger as the energy increases, in contrast to the behavior of a usual diffraction-type minimum. The reason for this is as follows. At the relatively high energies studied here

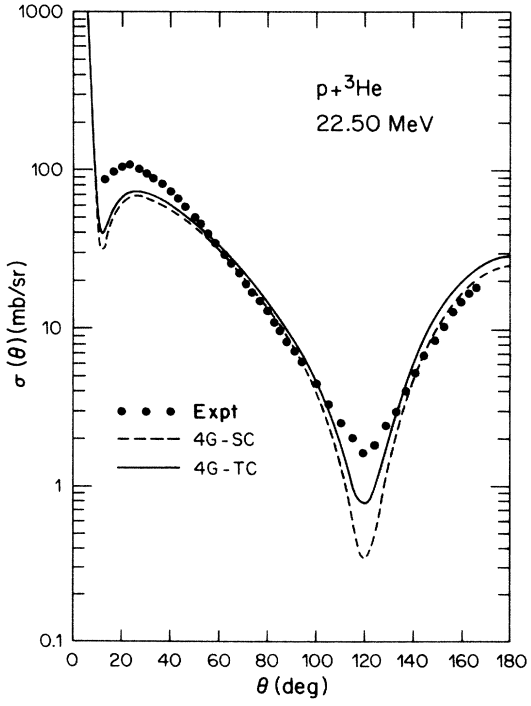

FIG. 5. Comparison of calculated differential cross sections for $p+^3He$ scattering at 22.5 MeV with experimental data.

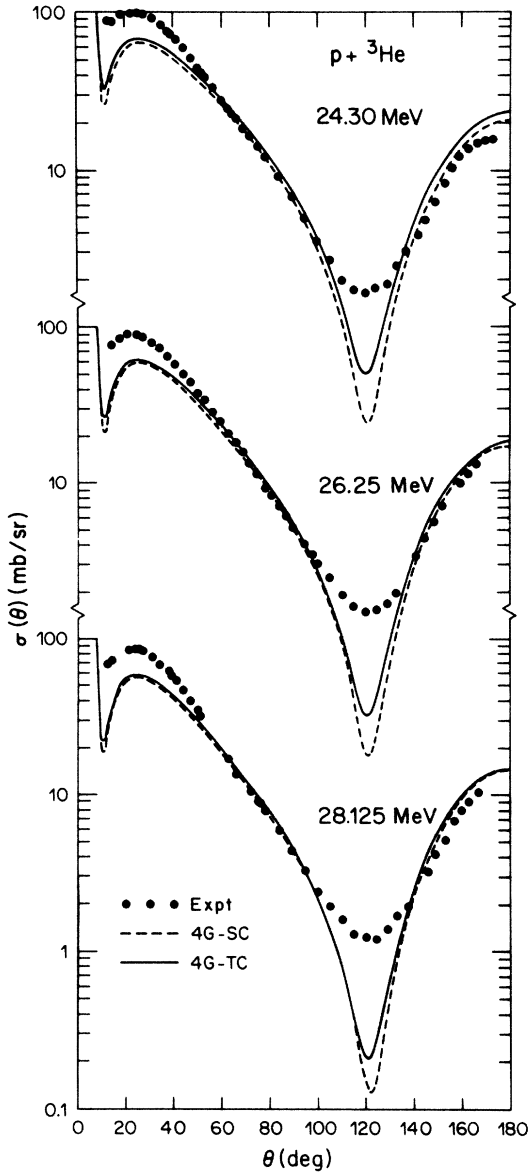

FIG. 6. Comparison of calculated differential cross sections for $p+^3He$ scattering at 24.30, 26.25, and 28.125 MeV with experimental data.

($E \geq 30$ MeV per nucleon), the contribution to the scattering amplitude in the forward angular region comes predominantly from the direct process and, to a much lesser extent, the one-exchange knockout process,[13] while the contribution to the scattering amplitude in the backward angular region comes almost entirely from the one-exchange heavy-particle pickup process (i.e., the neutron picks up a deuteron cluster). All these contributions become weaker as the energy becomes higher; however, the heavy-particle pickup amplitude decreases with increasing energy more rapidly than the direct amplitude, thus resulting in the observed phenomenon.

The rather slow increase of θ_{min} with energy indicates that the one-exchange contribution will remain important even at considerably higher energies. Therefore, it is anti-

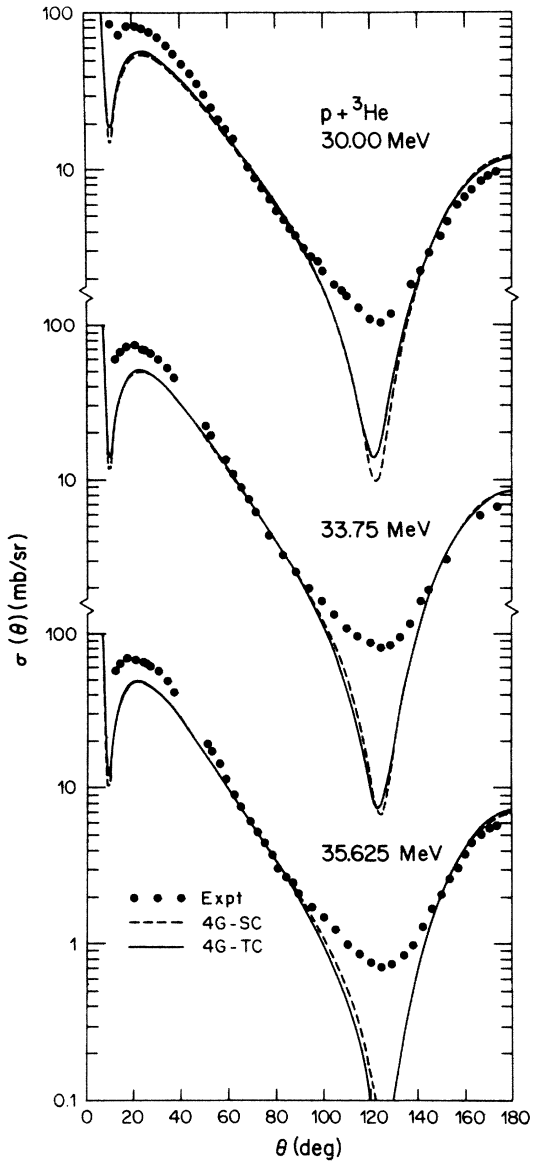

FIG. 7. Comparison of calculated differential cross sections for p+^{3}He scattering at 30.0, 33.75, and 35.625 MeV with experimental data.

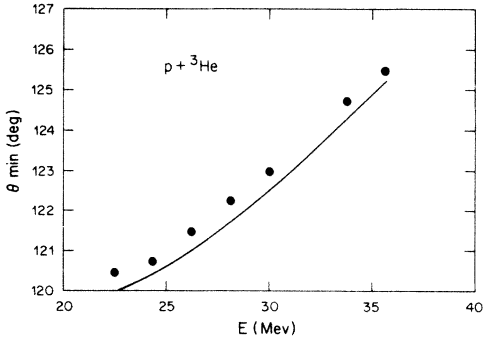

FIG. 8. Comparison of calculated angular positions of the cross-section minimum, caused by the interference between the direct amplitude and the one-exchange heavy-particle pickup amplitude, with experimental data.

cipated that the use of an optical model with conventional types of interaction potential will generally not yield a satisfactory explanation of the back angle data even when the energy is high. For a reasonable description of the data using a macroscopic model which does not take the Pauli principle explicitly into account, it seems clear to us that some crude representation of the exchange process,[14] such as the introduction of a Majorana component into the potential, must be employed.

V. CONCLUSION

In this investigation, the specific distortion effect of the three-nucleon cluster in the n + t or p+^{3}He system is studied by using the pseudostate method in the resonating-group formulation. The result indicates that such effect is significant mainly in the Pauli-favored $l=1$ state and, even in this particular orbital angular-momentum state, it is large only in the low-energy region around the broad resonance. At energies greater than 20 MeV, a comparison between differential cross-section results calculated with and without distortion shows quite clearly that, in the higher-energy region, the importance of this effect is rather minor.

Results from this study and a similar study in the t+α case show that the specific distortion of the triton cluster is appreciably more important in the t+α system than in the n + t system. This confirms one's intuitive feeling that the effect of specific distortion of a cluster is related not only to its own compressibility but also to the nucleon number of the companion cluster in the system.

The advantage of the pseudostate method lies in the fact that the kernel functions involved can be easily derived and the computation is straightforward. But there exist undesirable features as well. The presence of unphysical dispersionlike resonances complicates the interpretation and has the consequence that, at least in the n + t or p+^{3}He system, a comparison with experimental data cannot be made over a rather wide energy range. This type of defect can be sufficiently alleviated by utilizing a large number of pseudoinelastic configurations, but the requirement of computational time will then become severe. Rather, our opinion is that, for a detailed understanding of the effect of specific distortion, a better way is to carry out a more involved calculation employing realistic cluster configurations, such as the three-cluster n + n + d configuration.

This research was supported in part by the U.S. Department of Energy under Contract No. DOE/DE-AC02-79ER10364 and the Supercomputer Institute at the University of Minnesota.

[1]H. Jacobs, K. Wildermuth, and E. Wurster, Phys. Lett. **29B**, 455 (1969); D. R. Thompson and Y. C. Tang, Phys. Rev. C **8**, 1649 (1973); Z. C. Kuruoglu and F. S. Levin, Phys. Rev. Lett. **48**, 899 (1982).

[2]H. Kanada and Y. C. Tang, in Proceedings of the International Symposium on Few-Body Methods, Nanning, Quangxi, People's Republic of China, 1985.

[3]T. Nakamura, M.S. thesis, Niigata University, 1982.

[4]H. Kanada, T. Kaneko, S. Saito, and Y. C. Tang, Nucl. Phys. **A444**, 209 (1985).

[5]H. Kanada, T. Kaneko, and Y. C. Tang, Nucl. Phys. **A380**, 87 (1982); T. Kaneko, M. Shirata, H. Kanada, and Y. C. Tang (unpublished).

[6]D. R. Thompson, M. LeMere, and Y. C. Tang, Nucl. Phys. **A286**, 53 (1977).

[7]H. Kanada, T. Kaneko, and Y. C. Tang, Nucl. Phys. **A389**, 285 (1982).

[8]Y. C. Tang, M. LeMere, and D. R. Thompson, Phys. Rep. **47**, 167 (1978).

[9]M. Kamimura, Prog. Theor. Phys. Suppl. **62**, 236 (1977).

[10]Single-configuration calculations in $n=2$ to 6 cases yield nearly identical phase-shift values in the $(l,s)=(1,1)$ state.

[11]P. N. Shen, Y. C. Tang, Y. Fujiwara, and H. Kanada, Phys. Rev. C **31**, 2001 (1985).

[12]B. T. Murdoch, D. K. Hasell, A. M. Sourkes, W. T. H. van Oers, P. J. T. Verheijen, and R. E. Brown, Phys. Rev. C **29**, 2001 (1984).

[13]D. R. Thompson and Y. C. Tang, Phys. Rev. C **4**, 306 (1971).

[14]H. S. Sherif, M. S. Abdelmonem, and R. S. Sloboda, Phys. Rev. C **27**, 2759 (1983).